TAO, Vol. 8, No. 2, 213-220, June 1997

Traveling Ionospheric Disturbances Detected During the Solar Eclipse of 24 October 1995

Kang Cheng[1], Yinn-Nien Huang[2] and Sen-Wen Chen[1]

(Manuscript received 12 November 1996, in final form 19 March 1997)

ABSTRACT

During the total solar eclipse period on 24 October 1995, the ionospheric data derived from Faraday rotation, differential Doppler frequency shift, and HF Doppler sounding at Lunping Observatory were used to detect the traveling ionospheric disturbances associated with the solar eclipse of that day. These observed ionospheric disturbances were characterized by quasi-periodic wave-like trains lasting for several cycles with wavelengths of around 193 km, periods of around 12-14 min and propagated with a horizontal velocity of around 296 m/s from the direction of the eclipse path to the observation site. By use of a simplified bow wave front model, these traveling ionospheric disturbances are interpreted as the freely propagated atmospheric gravity waves generated by the supersonic movement of the Moon's shadow through the Earth's atmosphere along the eclipse path.

(Key words: Traveling ionospheric disturbances, Solar eclipse, Bow Wave Front Model)

1. INTRODUCTION

During the solar eclipse period, the cooling spot of the moon's shadow in the ozone layer at an altitude of about 45 km can be considered as a disturbance region in the lower atmosphere. The supersonic movement of the moon's shadow generates acoustic gravity waves (AG waves) along the eclipse path (Chimonas, 1970; Chimonas and Hines, 1970). These AG waves can be observed either as periodic pressure oscillations recorded by a microbarograph on the ground (Goodwin and Hobson, 1978), or as fluctuations of virtual height and critical frequency in ionograms and in total electron content measurements at a distance from the eclipse path (e.g. Cohen, 1984, and references therein).

On 24 October 1995, the total solar eclipse provided a good opportunity to study the characteristics of solar eclipse generated traveling ionospheric disturbances (TID's). At Lunping

[1]Directorate General of Telecommunications, MOTC, 16, Chinan Road, Taipei, Taiwan 100, R.O.C.
[2]Chunghwa Telecom Co. Ltd., MOTC, 31 Aikuo East Road, Taipei, Taiwan 106, R.O.C.

Observatory (25.00 ° N, 121.17 °E), the solar eclipse started at 1111LT, ended at 1354LT, and the maximum occultation occurred at 1233LT, with the eclipsed area of the solar disk being about 37% at an altitude of 300 km. The following are the observations made at Lunping Observatory during the October 24 1995 solar eclipse period:

(1) Continuous measurement of Faraday rotation of the linearly polarized VHF beacon signal at 136.38-MHz transmitted from GOES-3 geostationary satellite.

(2) Differential Doppler shift data, $d\Phi/dt$, measured by using the 150- and 400-MHz coherent signals transmitted from the US Navy Navigation Satellite System (NNSS) satellites (Huang and Cheng, 1991).

(3) Continuous HF Doppler shift data measured at a frequency of 7.8-MHz with transmitter stations located at Hsintien (24.94 °N, 121.52 °E), Keelung (25.09 °N, 121.87 °E), and Shihmen (25.28 °N, 121.56 °E); and a receiving station at Lunping (Huang *et al.*, 1985).

2. OBSERVATION RESULTS

Figure 1 shows the observed Faraday rotation during the afternoon period of the eclipse day. It is clear that the Faraday rotation exhibits a decaying phase of total electron content (TEC) diurnal variation. However after 1520LT, a distinct quasi-periodic oscillation of Faraday rotation lasting for two cycles superimposed on the decaying phase can be seen in the figure. Although the oscillation lasted for no more than two cycles, spectral analysis using the maximum entropy method (Ulrych and Bishop, 1975) shows that the period of the quasi-periodic Faraday rotation perturbations is approximately 14.3 min.

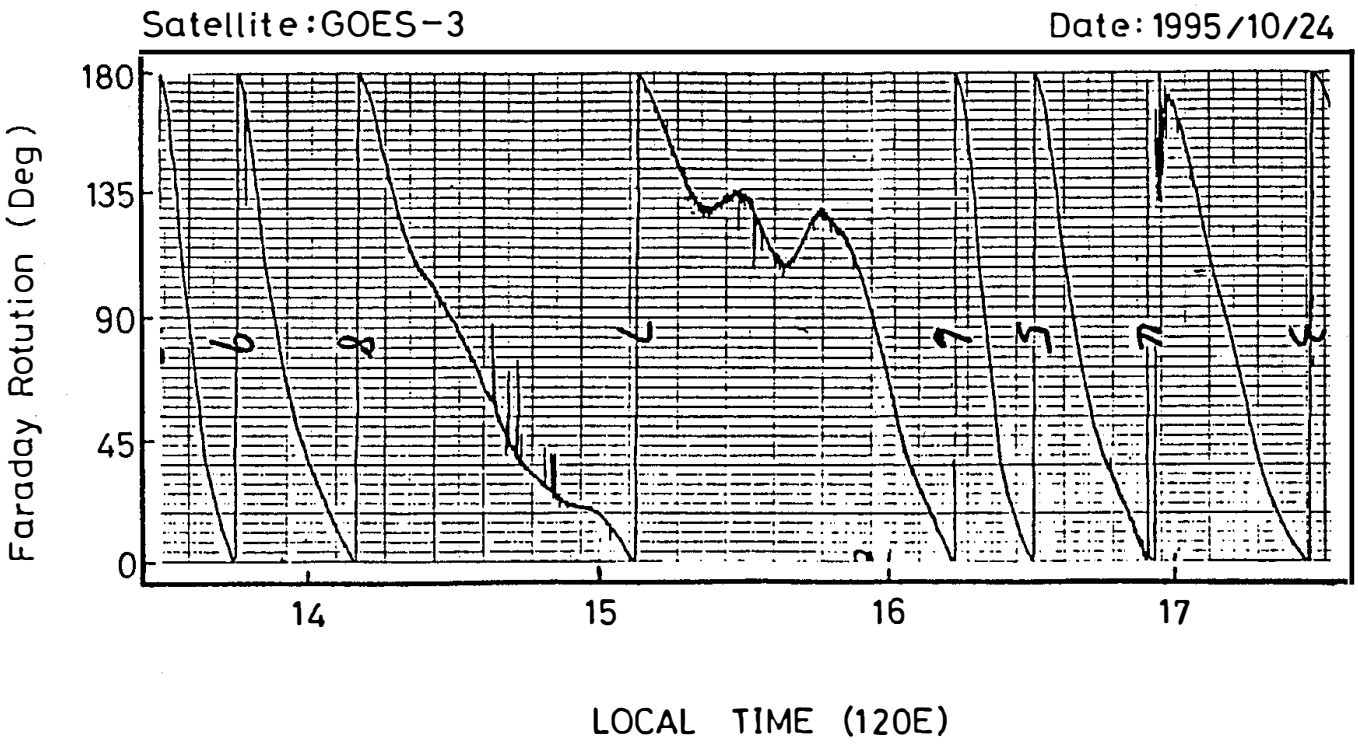

Fig. 1. Faraday rotation during the afternoon period of 24 October 1995.

After the solar eclipse, differential Doppler shift data, $d\Phi/dt$, obtained by receiving 150- and 400-MHz coherent signals transmitted from the US NNSS satellite, were available for three successive passages of the NNSS satellite during 1416-1432LT, 1516-1531LT and 1607-1618LT. Only the second passage (1516-1531LT), as shown in Figure 2, exhibits quasi-periodic fluctuations superimposed on the large latitudinal variation of the $d\Phi/dt$ curve. This is due to the development of a TEC equatorial anomaly near the equatorial anomaly crest (Huang and Cheng, 1991).

In order to eliminate the contribution of the TEC equatorial anomaly, a smoothed dotted curve derived from using the 12-point moving average of $d\Phi/dt$ is subtracted from the $d\Phi/dt$

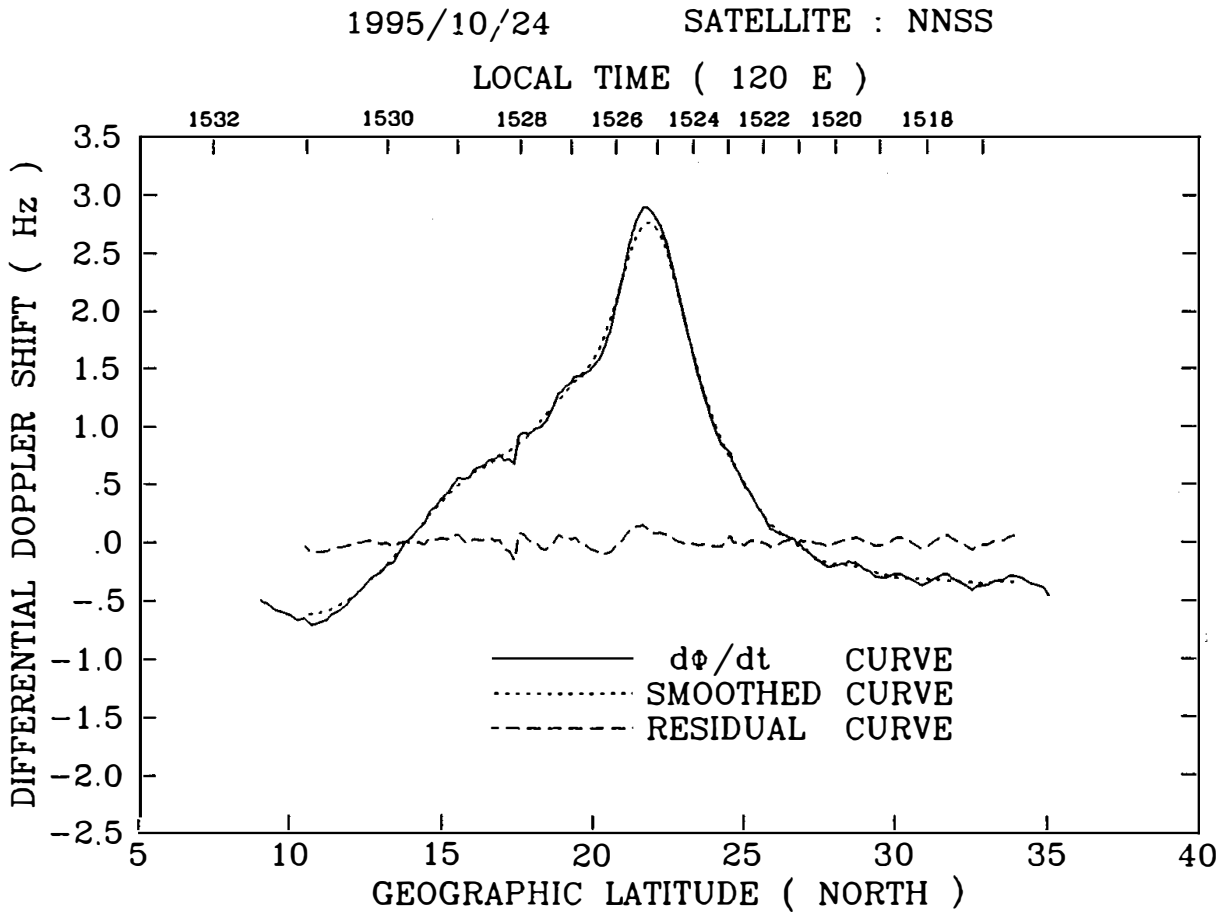

Fig. 2. Differential Doppler shift data showing quasi-periodic structure of ionospheric disturbances.

curve. The dashed curve in Figure 2 shows the residual value of $\Delta(d\Phi/dt)$. The residual curve reveals the fine structure of an atmospheric gravity wave covering the latitudinal region from 25 °N to higher than 35 °N. Since the maximum scanning time for a passage of the NNSS satellite is not more than 15 min and its traveling velocity (~7.4 km/s) is much faster than the propagation velocity of traveling ionospheric disturbances (< 1 km/s), the observed ionospheric wavelike fluctuations can be considered to be a real stationary ionospheric quasi-

periodic structure (Evans *et al.*, 1983), with a wavelength of about 193 km.

Figure 3 shows the band-pass filtered (6-30 min) HF Doppler shift data obtained at 7.8 MHz from 1000-1800LT on the eclipse day. Quasi-periodic fluctuations lasting for several cycles can be seen between 1430-1520LT, as indicated by a horizontal bar. Spectral analysis, using the data obtained during 1430-1520LT, shows that it has a period of around 12 min. Using cross correlation analysis and triangulation, the horizontal phase velocity and the azimuth of the propagation direction for the quasi-periodic oscillations were determined as 296 m/s and 24 °, respectively. Taking this propagation velocity and the perturbation period, the horizontal wavelength of the perturbation can be estimated to be about 213 km.

3. SUMMARY AND DISCUSSION

During the total solar eclipse period on 24 October 1995, quasi-periodic TID's were observed in the Faraday rotation data, the differential Doppler shift data, and the HF Doppler sounding data measured at Lunping Observatory. These TID's are characterized by a wavelength of around 193 km, a period of around 12-14 min, and propagate with a horizontal velocity of around 296 m/s from the direction of the eclipse path to the observation site. The characteristics of the TID's observed during the solar eclipse period on 24 October 1995 are

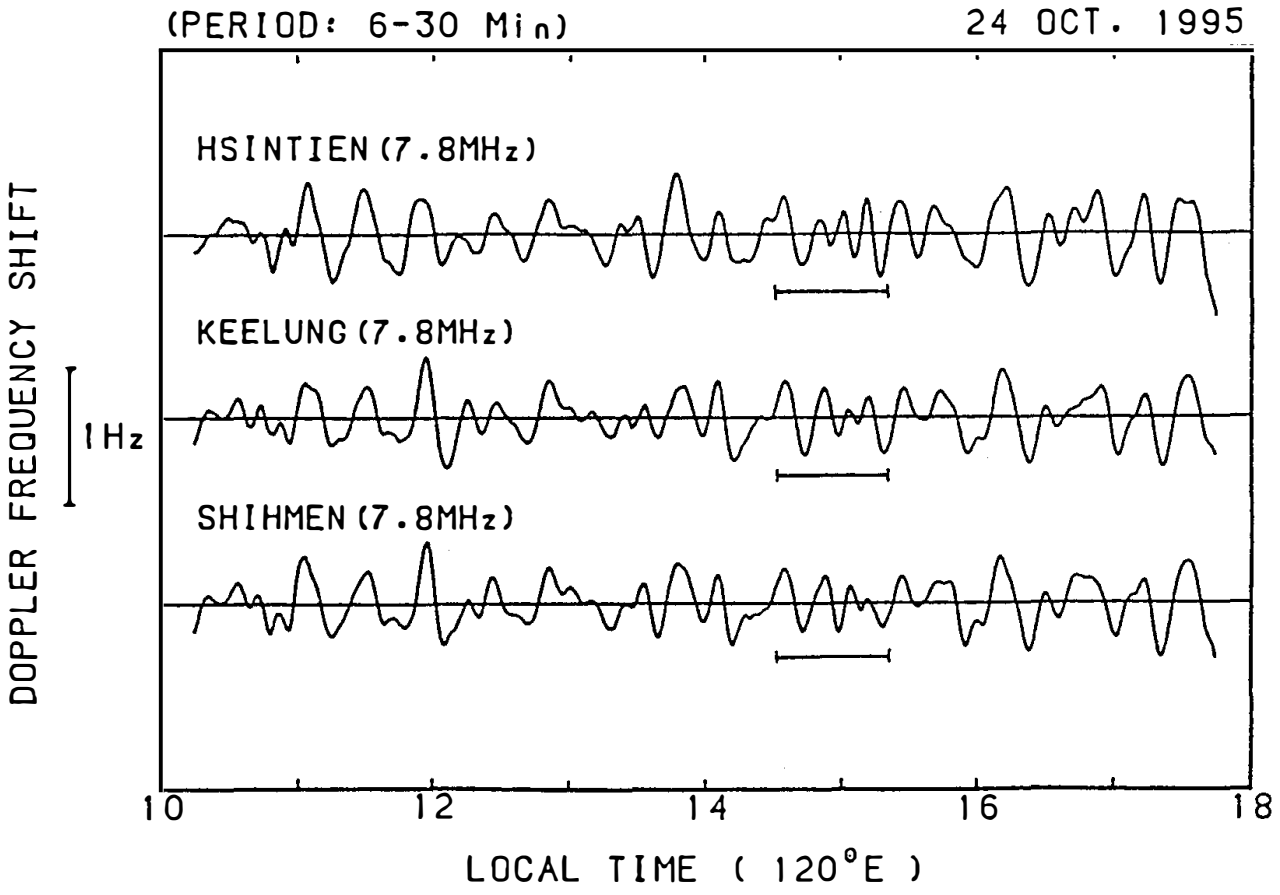

Fig. 3. Band-pass filtered (6-30 min) HF Doppler shift data.

Table 1. Characteristics of traveling ionospheric disturbances observed after the solar eclipse on 24 October 1995.

	Wavelength	Period	Velocity	Time of Detection	Distance from Eclipse Path
Faraday Rotation	- - -	14,3 min	- - -	1520 -1550 LT	2590 km
Differential Doppler Frequency Shift	193 km	- - -	- - -	1516 - 1520 LT	2260 - 3200 km
HF Doppler Frequency Shift	213 km	12 min	296 m/s	1430 - 1520 LT	2260 km

- - - indicates observation data not a vailable

listed in Table 1. The detection times of TID's and the distances from the eclipse path to where the data are measured are also listed in the Table.

Based on the localized cooling spot caused by the moon's shadow near the peak of ozone absorption of solar X-ray and UV radiation, which occurs at an altitude of about 45 km, Chimonas and Hines (1970) and Chimonas (1970) developed the theory of an eclipse-induced gravity wave during the solar eclipse period. It is suggested that when the moon's shadow moves at supersonic speed across the atmosphere, the gravity waves will propagate freely with an oblique path to the ionospheric heights in the form of a bow wave front in the wake of the shaded region.

In an attempt to find an association between the observed TID's and the eclipse, a simplified model has been developed for the propagation of eclipse generated TID's and the observations are tested against this. The model uses the concept of a bow wave front, generated when a source is moving faster than the characteristic speed of waves in the medium through which it is traveling, where the angle of the bow wave front to the source direction is determined by the source speed and the characteristic wave speed (Chimonas, 1970; Chimonas and Hines, 1970).

In Figure 4 the thick solid dotted curve AB represents the eclipse path. The center of the moon's shadow at each 5-min interval is indicated as a dot on the eclipse path. The speed of the moon's shadow is determined by Nautical Almanac Office (1994). The thin solid curves show the locations of the corresponding bow wave front at each 15-min interval at the characteristic speed of 245 m/s. The dashed curves indicate the ray paths of the bow wave front along great circles. The asterisks indicate the locations of Lunping Observatory (LNP) and the GOES-3 subionospheric point. The track of the subionospheric point of NNSS satellite is shown as a chained curve in Figure 4. The hatched part of the NNSS track indicates the region where the atmospheric gravity wave is observed. Comparing the detection times of the TID's listed in Table 1 with the locations of the bow wave front, it is interesting to note that the

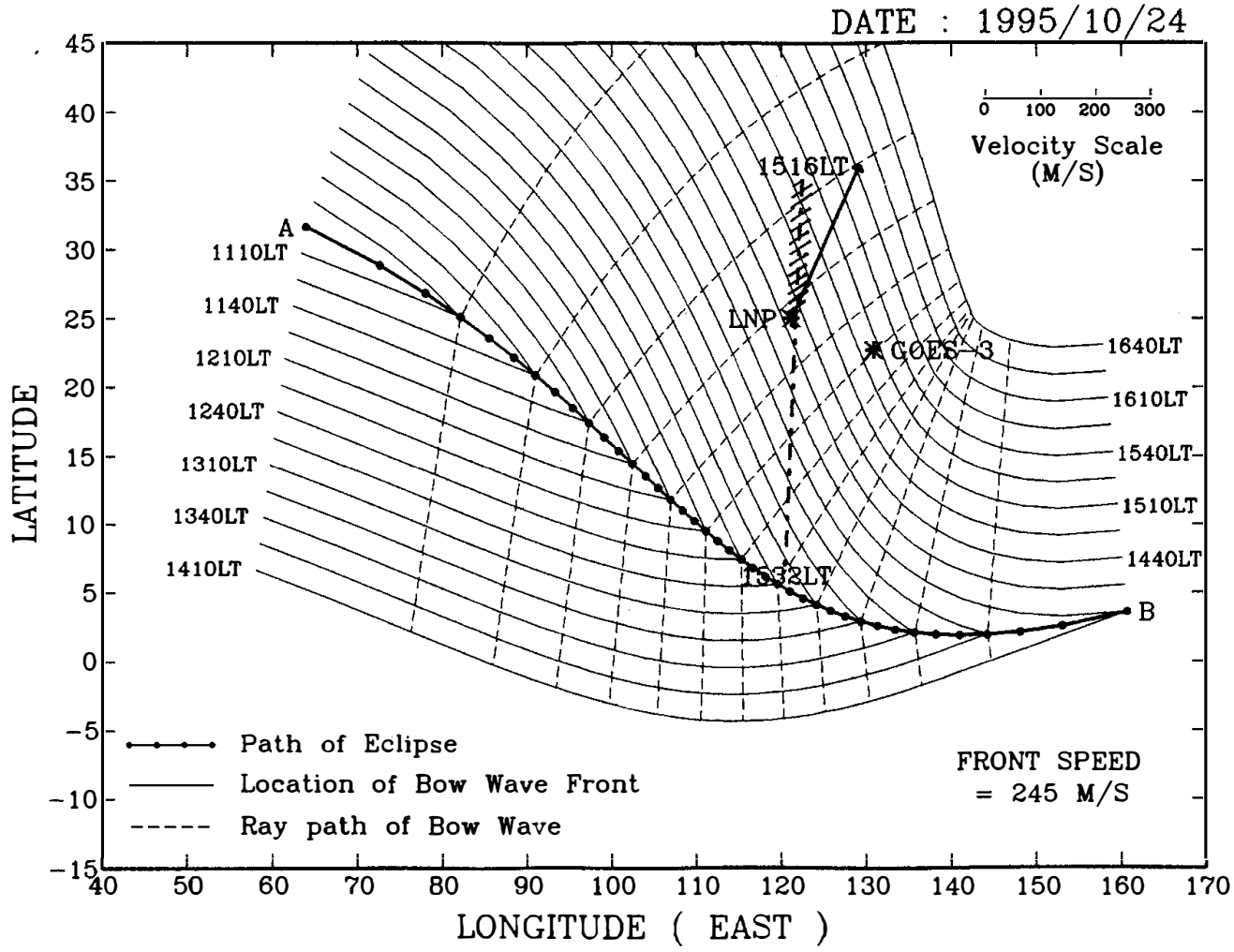

Fig. 4. Simplified bow wave front model. The horizontal propagation vector determined from HF Doppler Network and the track of NNSS satellite detected quasi-periodic fluctuations are also plotted in the figure.

Faraday rotation, the NNSS differential Doppler shift, and the HF Doppler sounding start respectively to observe the quasi-periodic fluctuation at the same time and the same location as the bow wave front arrives. On the other hand, from this bow wave front model, the TID's generated by the supersonic motion of the moon's shadow reach the site of HF Doppler sounding earlier than the site of Faraday rotation, as observed.

The horizontal propagation velocity vector determined from the HF Doppler shift sounding is also plotted in Figure 4, as an arrow. Comparing the direction of the velocity vector with that of the ray path of the bow wave front, it is also suggested that the AG waves detected by the Doppler shift sounding are generated by the supersonic movement of the moon's shadow and propagate to Taiwan. In the realistic atmosphere, where the gravity waves propagate from the source in the upper troposphere to the ionospheric heights where the disturbances are observed, the gradient of background atmosphere may reflect or refract the waves, and the horizontal background wind in the stratosphere and the mesosphere can act as a directional

filter (Yeh and Liu, 1974). The deviation of the observed propagation velocity and direction from those derived from the simplified bow wave front model may be as a result of the horizontal background wind.

Experimental analysis in the realistic atmosphere (Row, 1967) and theoretical study in an isothermal atmosphere (Francis, 1975) show that the freely propagated gravity waves detected at the ionospheric height will accelerate as they move away from the source, and will have periods of oscillation proportional to the observer's distance from the source. From Table 1, it can be seen that the ionospheric perturbation period increases from 12 min, as derived from HF Doppler shift data, to 14.3 min, as derived from Faraday rotation data, with the ratio being 1.19. This ratio is consistent with the ratio between the distances from the eclipse path to where the data are measured, i.e. 2590/2260 = 1.15. This implies that the TID's observed during eclipse period are propagated freely from the source region on the eclipse path to the observation sites.

The results of this study suggest that the traveling ionospheric disturbances detected in the Faraday rotation, differential Doppler frequency shift, and HF Doppler sounding at Lunping Observatory were manifested by the freely propagating gravity waves which were generated by the supersonic motion of the moon's shadow through the Earth's atmosphere along the eclipse path, and propagated upward to the ionosphere around the equatorial anomaly region.

REFERENCES

Chimonas, G., 1970: Internal gravity wave motions induced in the Earth's atmosphere by a solar eclipse. *J. Geophys. Res.*, **75**, 5545-5551.

Chimonas, G. and C. O. Hines, 1970: Atmospheric gravity waves induced by a solar eclipse. *J. Geophys. Res.*, **75**, 875-876.

Cohen, E. A., 1984: The study of the effect of solar eclipses on the ionosphere based on satellite beacon observations. *Radio Sci.*, **19**, 769-777.

Evans, J. V., J. M. Holt and R. H. Wand, 1983: A differential Doppler study of traveling ionospheric disturbances from Millston Hill. *Radio Sci.*, **18**, 435-451.

Francis, S. H., 1975: Global propagation of atmospheric gravity waves: A review. *J. Atmos. Terr. Phys.*, **37**, 1011-1054.

Goodwin, G. L. and G. J. Hobson, 1978: Atmospheric gravity waves generated during a solar eclipse. *Nature*, **275**, 109-118.

Huang, Y. N. and K. Cheng, 1991: Medium-scale traveling ionospheric disturbances around the equatorial anomaly crest as detected by the differential Doppler shift method. *J. Atmos. Terr. Phys.*, **53**, 619-626.

Huang, Y. N., K. Cheng and S. W. Chen, 1985: On the detection of acoustic-gravity waves generated by typhoon by use of real-time HF Doppler frequency shift sounding system. *Radio Sci.*, **20**, 897-906.

Nautical Almanac Office, 1994: The astronomical Almanac 1985. US Government Printing Office, Washington, D. C.

Row, R. V., 1967: Acoustic-gravity waves in the upper atmosphere due to a nuclear detona-

tion and an earthquake. *J. Geophys. Res.*, **72**, 1599-1610.

Ulrych, T. J. and T. N. Bishop, 1975: Maximum entropy spectral analysis and autoregression decomposition. *Rev. Geophys.*, **13**, 183-200.

Yeh, K. C. and C. H. Liu, 1974: Acoustic-gravity waves in the upper atmosphere. *Rev. Geophys.*, **12**, 193-216.